The TELFLOOD Project, estimation of precipitation over drainage basins.

Stefan Gollvik

The TELFLOOD Project, estimation of
precipitation over drainage basins.

Stefan Gollvik

Cover photo:
Stefan Gollvik, "Blåfjellet in August"

Report Summary / Rapportsammanfattning

Issuing Agency/Utgivare	Report number/Publikation
Swedish Meteorological and Hydrological Institute S-601 76 NORRKÖPING Sweden	RMK No. 77
	Report date/Utgivningsdatum June 1997

Author (s)/Författare

Stefan Gollvik

Title (and Subtitle)

The TELFLOOD Project, estimation of precipitation over drainage basins

Abstract/Sammandrag

We have been doing precipitation experiments with a numerical weather prediction model. The model has been run with three different horizontal resolutions, 22, 11 and 5 km respectively. The results show that the model is able to forecast reasonable precipitation amounts in a broad sence, but it has difficulties to estimate the correct amount over small drainage basins. No significant improvements can be seen, when the higher horizontal resolutions are used. The results are sensitive to the magnitude of the horizontal diffusion, which is used in the model to control the horizontal spectra.

For orographically enhanced areas the result is much better, but also in these cases the higher resolution forecasts have to be strongly damped in order not to create noisy precipitation patterns. It is shown that smoothing the orography instead of a strong horizontal diffusion gives more realistic precipitation. It is suggested to compute the tendencies of the physical parameterization on a coarser grid than that of the dynamics.

Key words/sök-, nyckelord

precipitation, horizontal diffusion, numerical model, orography, drainage basin

Supplementary notes/Tillägg	Number of pages/Antal sidor 25	Language/Språk English

Report available from/Rapporten kan köpas från:

SMHI
S-601 76 NORRKÖPING
Sweden

TABLE OF CONTENTS

The TELFLOOD Project, estimation of precipitation over drainage basins.

Stefan Gollvik, SMHI, Sweden

1. Introduction

It is of great importance to get information about the expected precipitation and its distribution in time and space. Large rainfalls in combination with wet soils can occasionally give rise to flooding. It is of great help to the society and for the hydro power industry in particular to know these events beforehand.

The purpose of the TELFLOOD project is to try to estimate when flooding is likely to appear, i.e. to develop methods for forecasting on the timescale of 12-24 h. It means that the forecasting system shall contain both meteorological and hydrological components. For the meteorological part, the purpose is to give quantitatively good precipitation forecasts, over relatively small drainage basins.

There are several reasons, why it is difficult to estimate the precipitation. Even measuring the amount of precipitation over a drainage basin, is far from a straight forward task. The precipitation is characterized by small scales both in time and space, and the in situ station measurements are normally too coarse. Precipitation measurements with radar are available, but are associated with serious uncertainties. The problem of mesoscale analysis, to produce gridded precipitation fields, which are consistent on a typical spatial scale has been treated in Häggmark et al., 1997.

For estimating the precipitation in forecast mode, we believe that the only available method is to utilize a complete three-dimensional numerical weather prediction model system. Therefore we have here concentrated on the precipitation that is produced by a numerical weather prediction model, in this case the HIRLAM-system (High Resolution Limited Area Model), which is documented in Källén, 1996. Here we have been using the version of HIRLAM, which is operational in Sweden (in all experiments we are using 24 vertical levels), with some small modifications (see below).

In HIRLAM the condensation parameterization utilizes the cloud water as a prognostic variable (Sundqvist et al., 1989, Sundqvist, 1993). This implies that the condensation scheme first produces cloud water, and this is then converted into precipitation, the process of which is modelled by using cloud physical assumptions. The cloud cover is diagnostically computed within the condensation scheme. The precipitation is either produced by convection, or by stratiform clouds, and it is assumed that convection is dominant, i.e. if the conditions for convection are fullfilled for a gridpoint, no stratiform clouds can be produced, except for convective anvils. The convection is based on the formulation of Kuo, 1974, which means that its intensity is a function of the convergence of water vapour.

2. Modifications to the HIRLAM-model

To make the condensation processes somewhat smoother some small changes in the parameterization of clouds and condensation processes were tried.

- Calculate the level of the convective cloudtop in a somewhat different way. Instead of demanding two consecutive levels of $T_c - T > 0$ (the temperature difference between the cloud and the environment) we demand a depth of 130 hPa.

- Introduce a relaxation time, τ, of *both* convective and stratiform cloudcover:

$$cucov_{new} = cucov_{old} + \frac{\Delta t}{\tau}\left(cucov_{new} - cucov_{old}\right)$$

$$stcov_{new} = stcov_{old} + \frac{\Delta t}{\tau}\left(stcov_{new} - stcov_{old}\right)$$

Here *cucov* and *stcov* mean convective and stratiform cloud cover respectively. τ is 30 min, but if $\frac{\partial cw}{\partial t} > 0$ in the convective case, τ is 10 min (*cw* is cloud water mixing ratio).

This means that both types of cloudcover can exist at the same time, and this should produce a more continuous cloud cover. Note that the cloud water is not touched.

3. Experiments over relatively weak orography

The precipitation of a gridsquare should be regarded as a mean value over that area. Often the drainage basin is rather small, which means that the precipitation is composed from a few grid-values only. This illustrates the problem of the sensitivity to the exact position of the forecasted precipitation. Overall numerical models can produce precipitation that is reasonable over an area, large enough to be described by many gridpoints, while the individual amount in each gridpoint can be of great uncertainty. However, in some places and situations, the local forcing of the orography might help to put the precipitation at the right spot.

We will study the effect on the precipitation of horizontal resolution, and compare the results, both to mesoscale analyses and point measurements. We have chosen a period from May 20 to 25 1996. The HIRLAM model has been run twice a day at 00Z and 12Z, up to +18h. The initial fields and the boundaries (every 6 hour) come from the Swedish operational 22 km analyses. We have verified the precipitation over two different drainage basins. One of them, Pepparforsen, is very small and it is situated in South-western Sweden, and the other is somewhat larger, Emån more to the east. These areas are shown in Figure 1, together with a part of the 22 km grid.
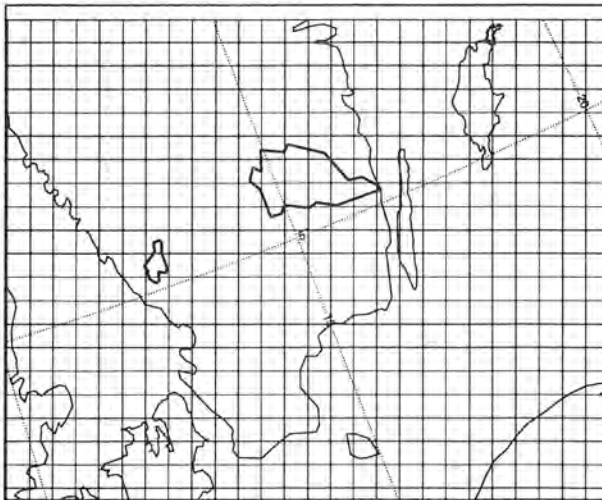

Figure 1. Two drainage basins in Southern Sweden.

The current precipitation measurements generally represent small areas, since the precipitation is a small scale phenomenon. When comparing model output data, which represent mean values over the gridsquares, it is reasonable to compare, not with point measurements, but instead with some analyses, which are more scale consistent in accordance with the spatial filtering characteristics of the analysis scheme. However, since the analyses are based on first guess fields from the model, some care has to be taken, and it is therefore important also to verify against 'pure' observations. For the smaller drainage basin, Pepparforsen, we have plotted, for every 12 hour, the 12h precipitation from May 20 at 18z until May 26 06z in Figure 2. Here we show two versions of the mesoscale analysed (14 km resolution) values over the drainage basins, one which is based on real time data (SYNOP) and another where also the climate station data are included (TOTAL), according to Häggmark et al., 1997. The latter is based on the observed 24h accumulated precipitation, but distributed to 12h values according to the synoptic information. Also the values that are used as input for the hydrological model (Lindström et al., 1996), based on some synop stations are shown. Here 'KORR' means the values after a correction according to height over sea level, and these are the values that normally are utilized by the hydrological model.

It can be seen from the figure that the observations and the analysed values are very similar. When comparing with actual forecasts, we will use the mesoscale analyses, which could be regarded as gridded precipitation data, filtered to a specific spatial scale.
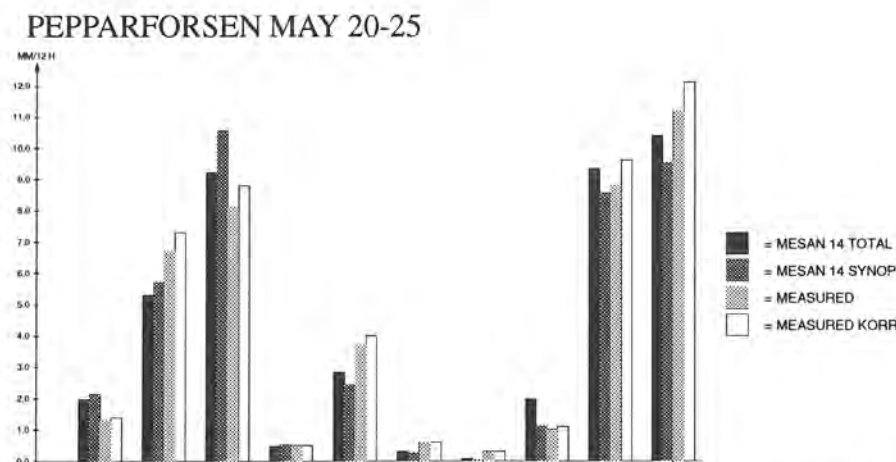
PEPPARFORSEN MAY 20-25

Figure 2. The 12h accumulated precipitation over Pepparforsen drainage basin, during May 20-25 1996.

In Figure 3 we are comparing the results of the 22 km HIRLAM forecasts with the mesoscale analyses. Here we have been running both 18h forecasts, and 24h forecasts with the precipitation from +6h and +12h respectively. The two HIRLAM forecasts could be regarded as two perturbations of the initial state, and they show large differences in some situations.
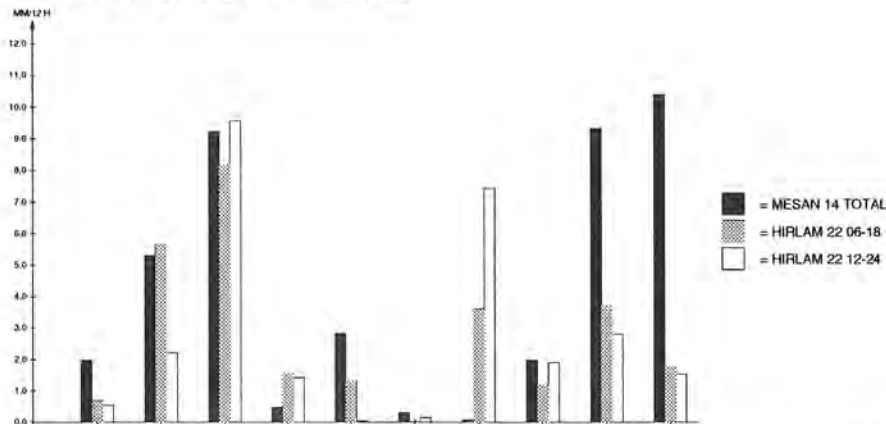
4

PEPPARFORSEN MAY 20-25

Figure 3. The 12h forecasted and analysed precipitation over Pepparforsen drainage basin, during May 20-25 1996.

In Figure 4 we compare the effect of different horizontal resolutions of the HIRLAM forecasts. They show big similarities in the beginning of the period, but at the end the precipitation of the 5.5 km run are somewhat higher, and comparable to the 22km longer forecast. This is however the case where the analysed precipitation is completely different. It is notable that the change of initial time produce differences as big as changing the resolution. No significant improvements are gained by increasing the resolution.

PEPPARFORSEN MAY 20-25
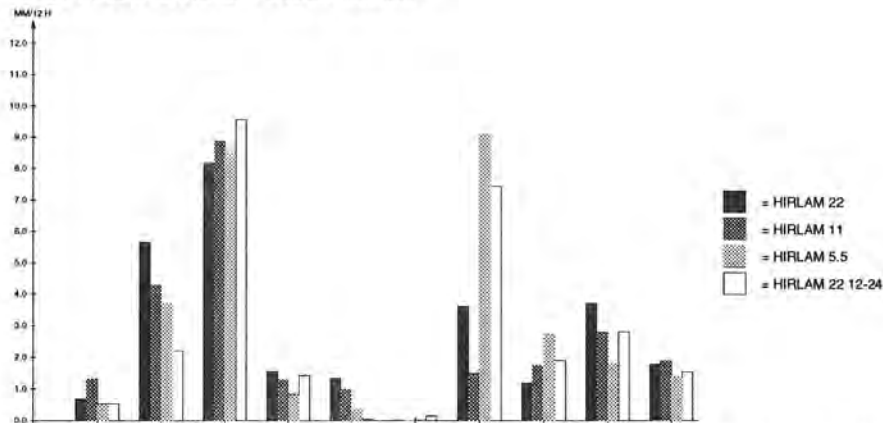
Figure 4. The 12h forecasted precipitation over Pepparforsen drainage basin, during May 20-25 1996, with different resolutions.

The corresponding figures for the somewhat larger drainage basin Emån are shown in Figure 5 and Figure 6. Here we can see a better correspondance, although the large analysed value in the beginning of the period is strongly underestimated in all the forecasts.
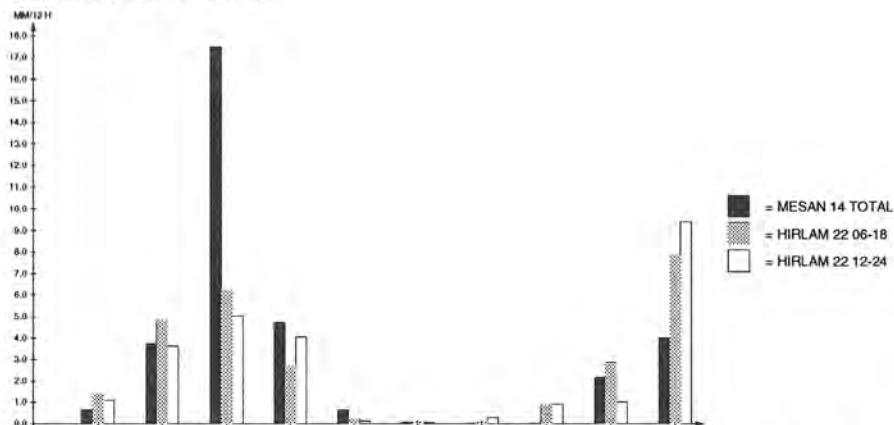
EMÅN MAY 20-25

Figure 5. The 12h forecasted and analysed precipitation over Emån drainage basin, during May 20-25 1996.
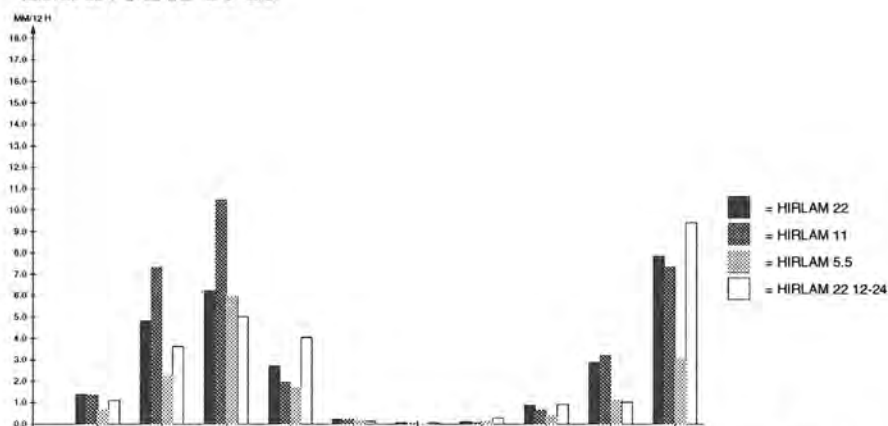
EMÅN MAY 20-25

Figure 6. The 12h forecasted precipitation over Emån drainage basin, during May 20-25 1996, with different resolutions.

We have looked more into detail on the case where the mesoscale analysis gave about 17 mm precipitation over the Emån basin, while the forecasts gave at most about 10 mm. In Figure 7 the mesoscale analysis of 12h precipitation at May 21 18z is shown.

6
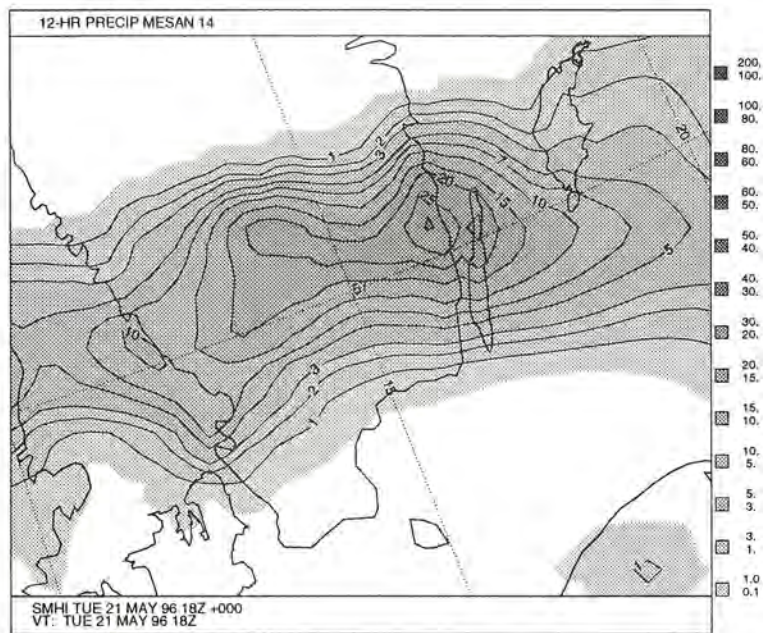
Figure 7. The 12h precipitation mesoscale analysis at May 21 18z.

The corresponding 22 km 18h precipitation forecast is shown in Figure 8. When comparing this forecast to the analysis, one can see that the overall forecast is good. However, over the Emån drainage basin the analysis shows a maxima of 30 mm, while the 22 km forecast shows less than 10 mm.

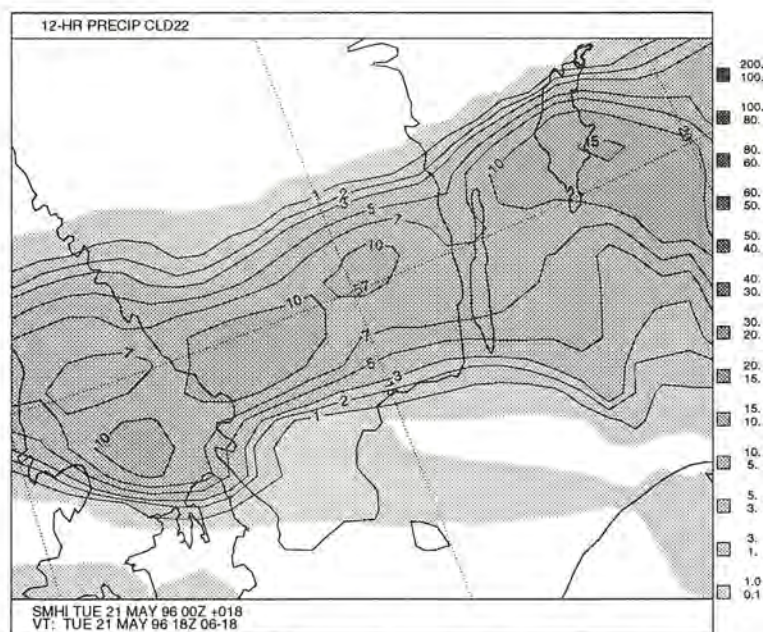The 11 km run gave about 10 mm over the drainage basin, and the forecast is shown in Figure 9.

Figure 8. The 12h precipitation from the 22 km +18h forecast at May 21 18z.
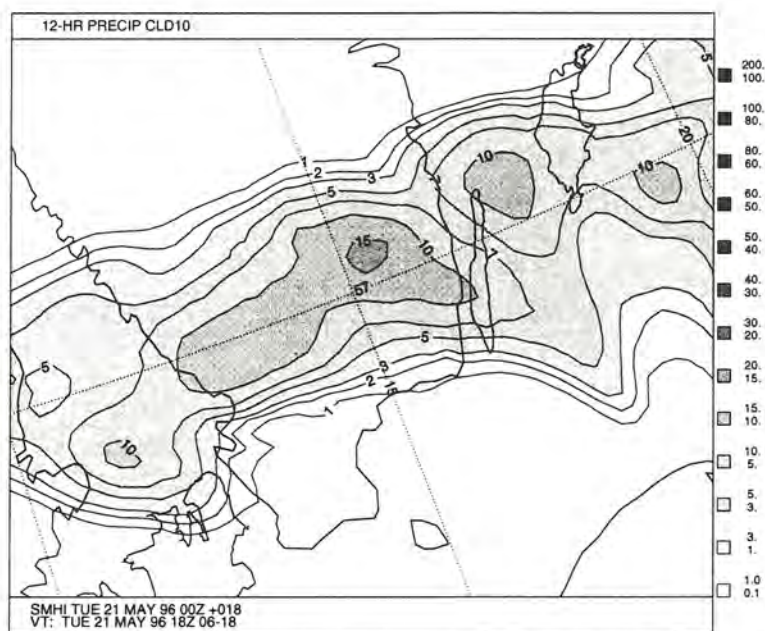
Figure 9. The 12h precipitation from the 10 km +18h forecast at May 21 18z.

This precipitation pattern of this 11 km forecast is very smooth, and this is due to the horizontal diffusion, which is included in the HIRLAM model, see Gustafsson and Mc Donald, 1996. Formally the fourth order horizontal diffusion can be written as:

$$\frac{\partial \Psi}{\partial t} = k \nabla^4 \Psi$$

where k is the diffusion coefficient. In Figure 10 and Figure 11 are shown the kinetic energy spectra for the 22 km and the 11 km forecasts respectively. The diffusion coefficient has been chosen to $6. * 10^{12}$ for the 22 km case, and to $1.2 * 10^{13}$ for the 11 km case. The timestep was 7.5 minutes for the 22 km run and 3 minutes for the 11 km forecast. This implies an e-folding damping time for the 4-gridlength wave of 110 minutes and 5 minutes respectively.
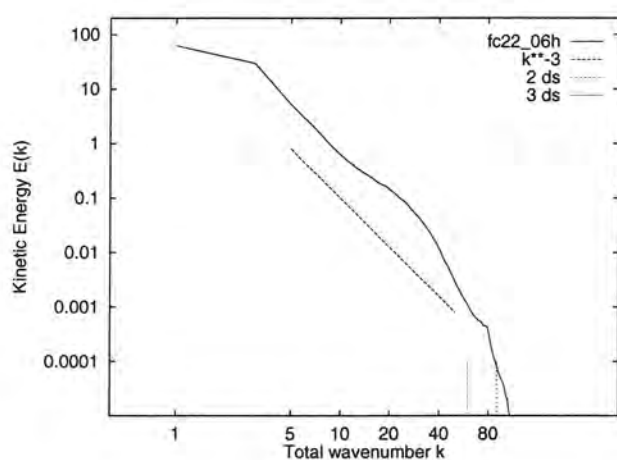

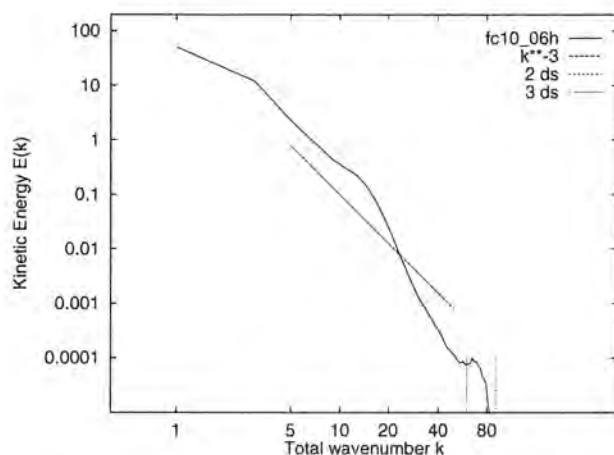Figure 10. The kinetic energy spectrum for the 22 km forecast.

Figure 11. The kinetic energy spectrum for the 11 km forecast.

In the figures also the line corresponding to a -3 slope is shown as a comparison. The 11 km run is too strongly damped in the shortest waves, and therefore we have also rerun this forecast with a smaller coefficient of the horizontal diffusion, i.e. $6. * 10^{11}$ corresponding to a damping time of the 4-gridlength wave of about 68 minutes. The corresponding 11 km precipitation is shown in Figure 12 and the energy spectrum in Figure 13.
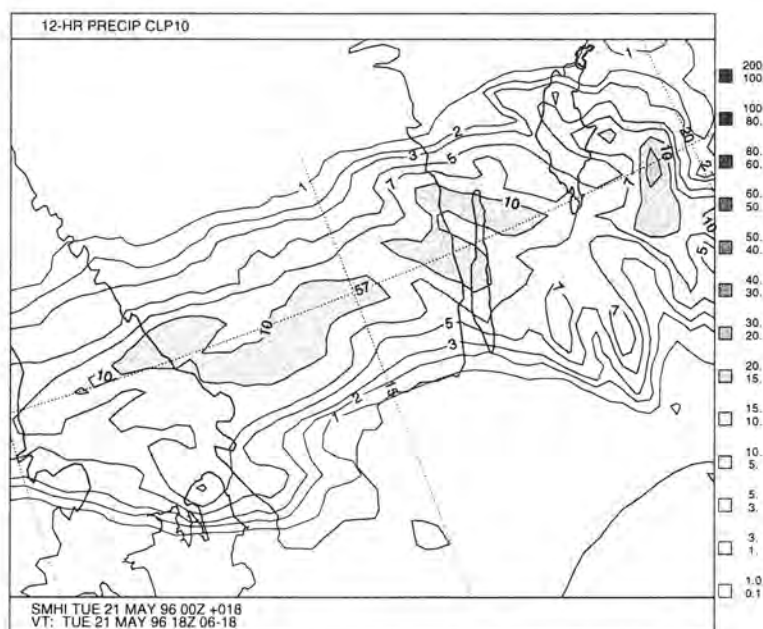

Figure 12. The 12h precipitation from the 11 km +18h less damped forecast at May 21 18z.
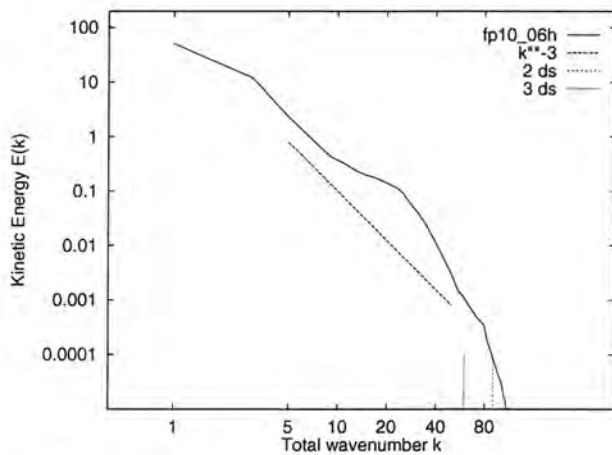
Figure 13. The kinetic energy spectrum for the less damped 11 km forecast.

Here we can see that the precipitation pattern is more noisy and, on the other hand, that the kinetic energy spectrum looks more reasonable than in the more damped case.

We have also looked at the 5 km forecast of this case and we have tried three different horizontal diffusion parameters. In Figure 14 we have the strongly damped case that was used in the series of forecasts shown earlier ($k = 1.2 * 10^{13}$). The corresponding energy spectrum is shown in Figure 15.
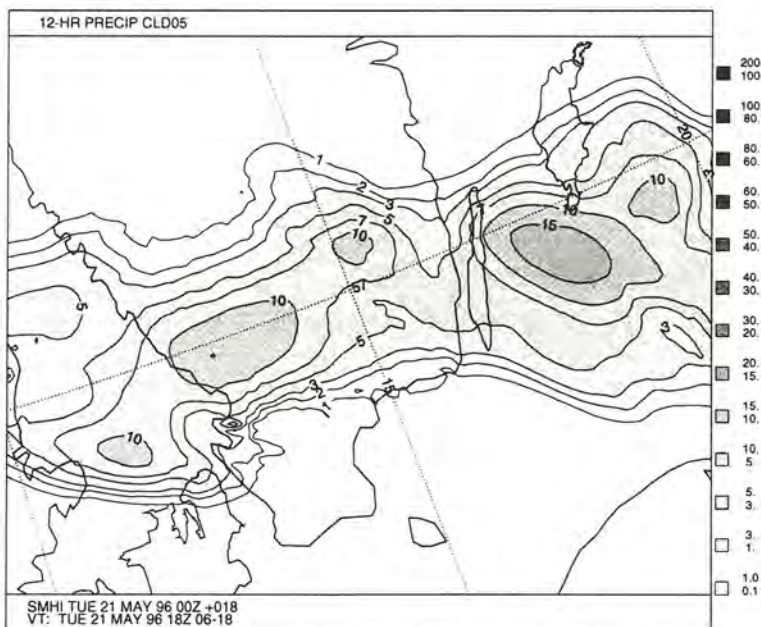

Figure 14. The 12h precipitation from the 5 km +18h forecast at May 21 18z.
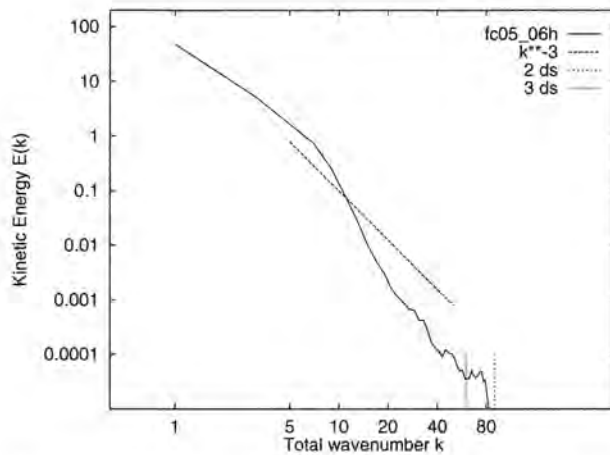
Figure 15. The kinetic energy spectrum for the 5 km forecast.

The damping is very strong in this case, the forecast is rather smooth and the precipitation pattern is similar to the 22 km case, although a strong maximum south west of Gotland is present here.

A somewhat less damped version of the 5 km forecast and the corresponding energy spectrum ($k = 3. * 10^{12}$) are shown in the Figures 16 and 17. Here the energy spectrum has relatively less energy in the shorter resolved waves than is the case of the 22 km forecast, but a larger damping is needed, to get reasonable precipitation patterns, when the scales are smaller. An alternative test with less horizontal diffusion produced a very noisy precipitation pattern, but it is not clear how the optimum values of these parameters shall be tuned.
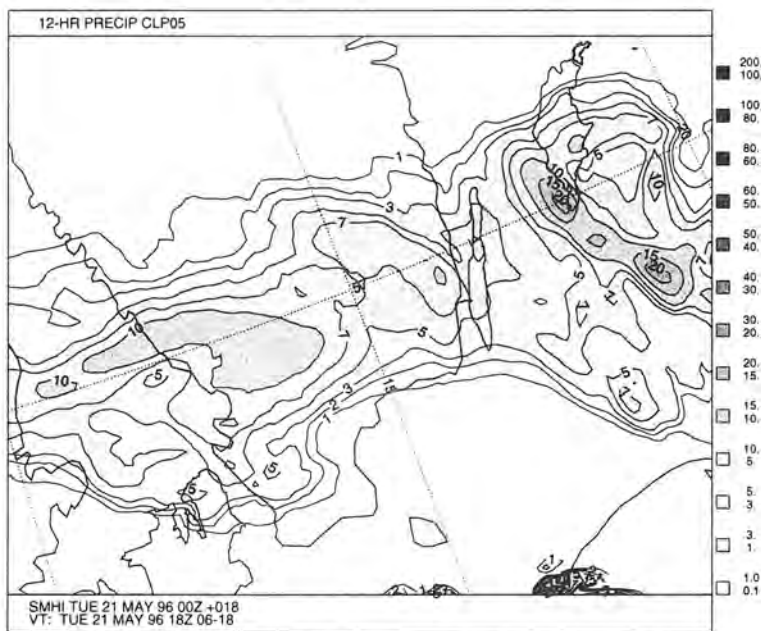

Figure 16. The 12h precipitation from the less damped 5 km +18h forecast at May 21 18z.
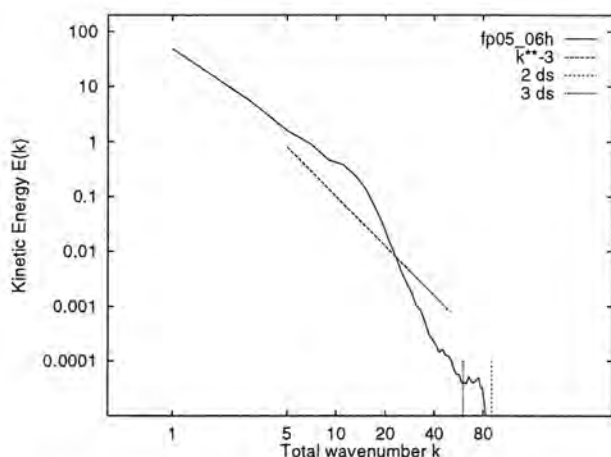
Figure 17. The kinetic energy spectrum for the less damped 5 km forecast.

It is not obvious, whether the small scale pattern that is produced by higher horizontal resolution, is realistic or spurious. We have compared the result from two 18h forecasts of 12h precipitation, thus estimating a 24 h value in the morning on May 22 at 06z. These forecasts have been compared to climatic stations, i.e. completely independent data. Here we are comparing point measurements to grid averages, but it should be possible to estimate at least differences between the different experiments. Of course it can be expected that high values are underestimated, due to the small scale of large precipitation amounts. In these comparisons all trivial cases are taken away, i.e. the cases where both the forecast and the measurement are zero.

In Figures 18 and 19 scatter diagrams for the 22 km and 11 km run are shown. The 11 km case is the strongly damped version, and this is the forecast that gave the best objective scores. There are no significant differences between the two cases, although a smaller scatter, especially for the smaller values, can be seen in the 11 km case.
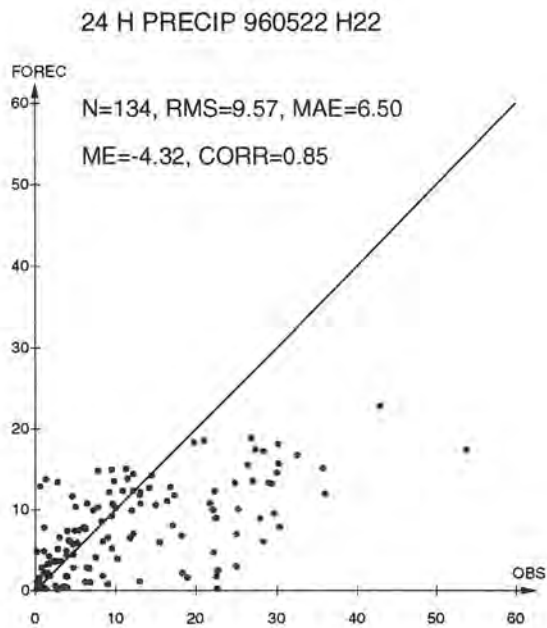
12

24 H PRECIP 960522 H22

Figure 18. 22 km forecasts:
Verifications against climate stations 24h acc. prec at May 22 06z.
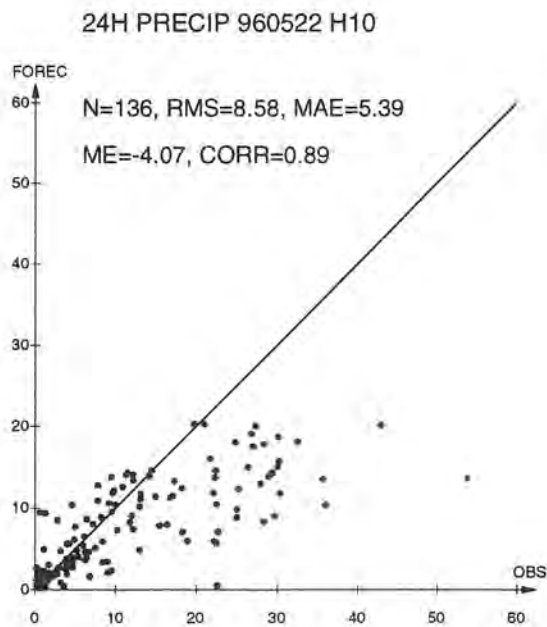
24H PRECIP 960522 H10

Figure 19. 11 km forecasts:
Verifications against climate stations 24h acc. prec at May 22 06z.

The less damped 11 km and 5 km runs are shown in Figures 20 and 21. It is a little surprising that this 11 km run doesn't show a better skill than that of Figure 19. The small scale features of the 5 km runs are not enough correctly described to improve the forecasts. In all cases we can see an underestimation of larger values. This could, as discussed above, partly be explained due to the small scale features of the precipitation.

24 H PRECIP 960522 H10 P
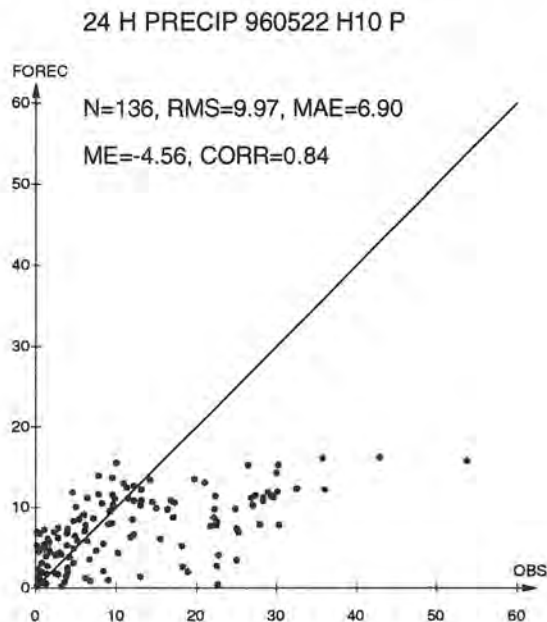

Figure 20. 11 km less damped forecasts:
Verifications against climate stations 24h acc. prec at May 22 06z.
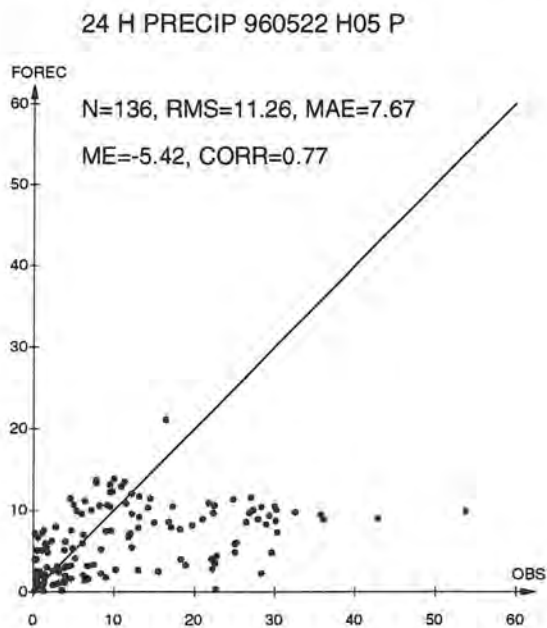
24 H PRECIP 960522 H05 P

Figure 21. 5 km less damped forecasts:
Verifications against climate stations 24h acc. prec at May 22 06z.

The experiments described above do not show any improvements, when the horizontal resolution is increased. The initial fields and boundaries of the 11 km and 5.5 km runs are interpolated from the 22 km analyses. The orography is of course produced from higher resolution data. One possible explanation for the lack of improvements could be the so called *spin up* problem. The 22 km forecasts should be better in this respect, since no interpolation is done in these cases.

In the cases with higher resolution, where the area is smaller, it is possible that it is not sufficient to interpolate the boundaries between six hourly data. This means that the spin up problem could be more severe by this effect.

4. Experiments over strong orography

It is reasonable to assume that the results might be better if the flow is strongly influenced by orography, which could help in positioning the precipitation. Therefore we have made experiments during a period in June 1996, where we had some rainfall in the middle Scandinavia. The drainage basin used is Indalsälven. The orography and the drainage basin are shown in Figure 22, together with a larger verification area. This drainage basin is fairly large, which should be favourable in the respect of estimating the precipitation.
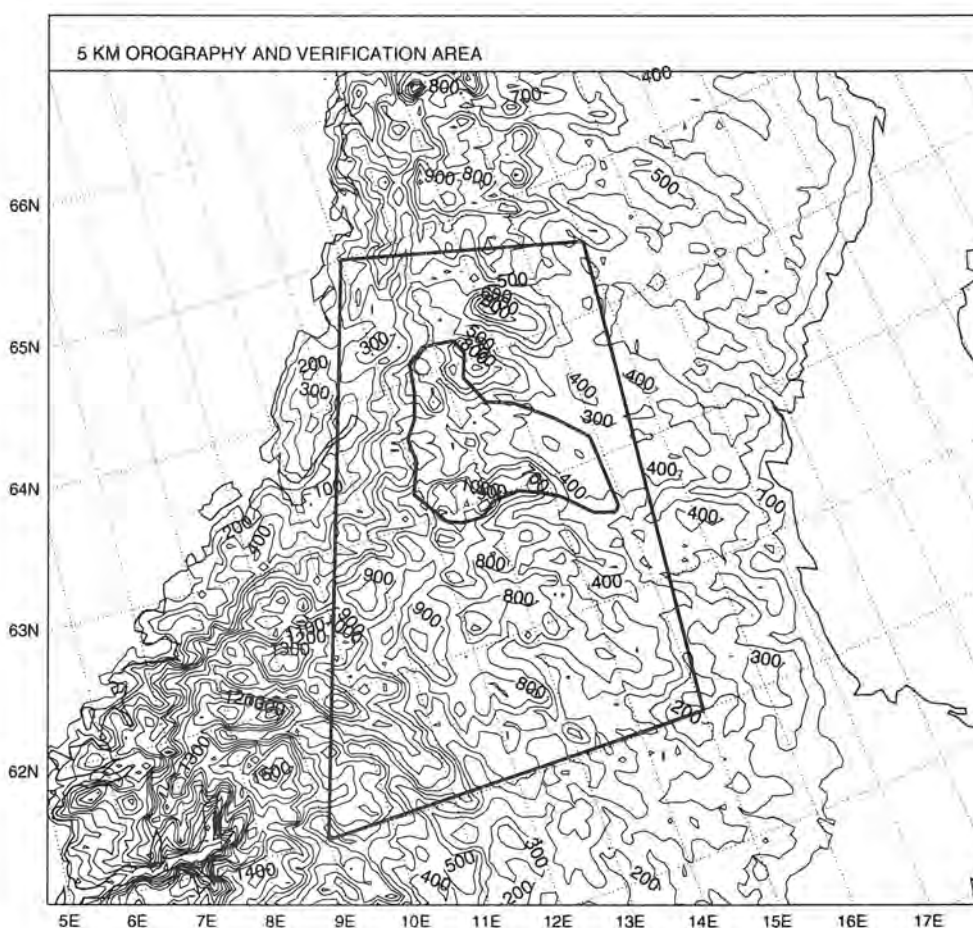

Figure 22. The 5.5 km orography in middle Scandinavia, the drainage basin Indalsälven and a larger verification area.

As before we have been running the HIRLAM model for three different resolutions. As discussed above, the results are dependent on the horizontal diffusion, and we have chosen values for 11 and 5.5 km, which give 'subjectively reasonable' precipitation patterns. Here we have used the same diffusion coefficient ($k = 6. * 10^{12}$) in all the experiments. This is is of course a weak point, since the results could differ for other diffusions. The 22 km and 5.5 km precipitations forecasts (+06h to +18h) for June 17 at 12Z are shown in Figures 23 and 24 respectively.
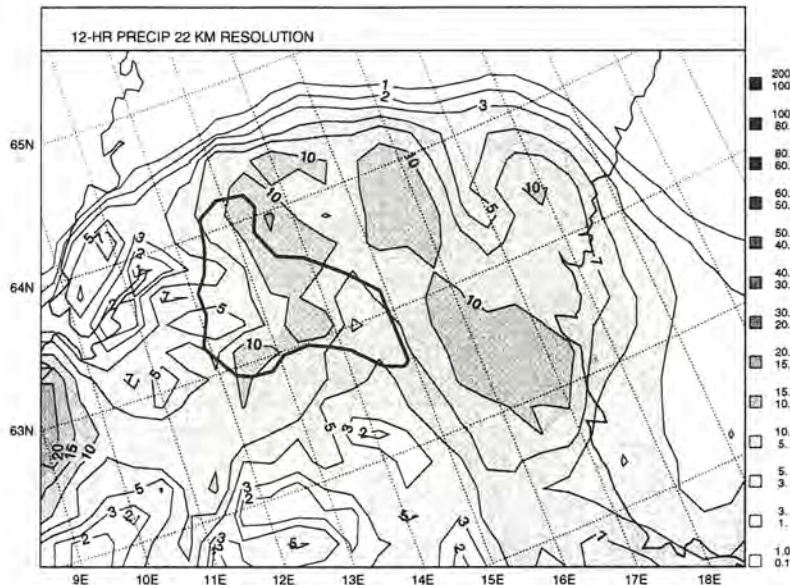

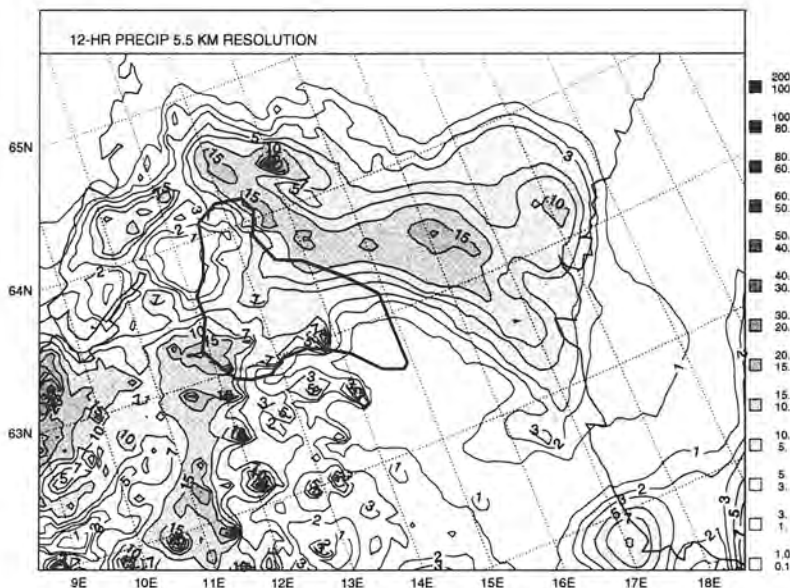Figure 23. The 12h precipitation from the 22 km +18h forecast at June 17 12z.

Figure 24. The 12h precipitation from the 5.5 km +18h forecast at June 17 12z.

16

The estimated values of the 24h precipitation over the drainage basin Indalsälven, for the period June 17 to 23 are shown in Figure 25. Here we show, as before the result of three different resolutions and also a mesoscale analysis. In this case this analysis is based on climate stations only. The number of stations within the drainage basin is about 20.
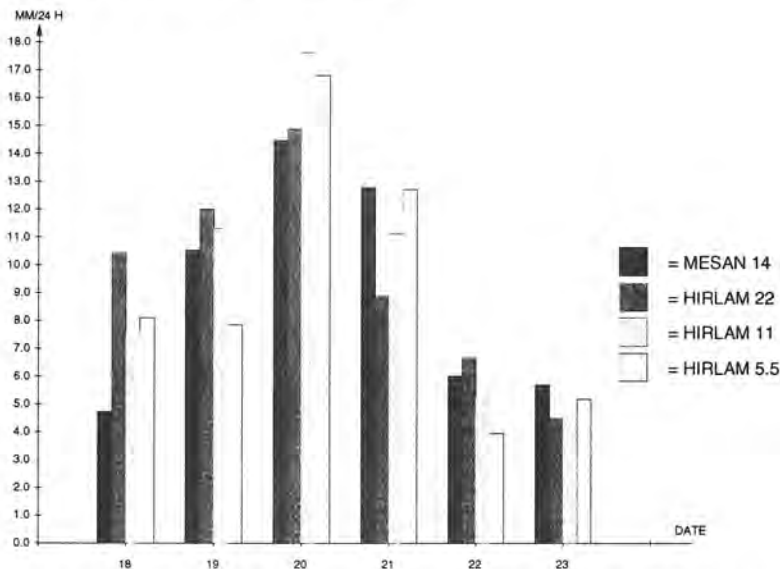
INDALSÄLVEN JUNE 18-23

Figure 25. The 24h accumulated precipitation over Indalsälven drainage basin, during June 17-23 1996.

It can be seen from the figure that most of the forecasts are much better in this case, as compared to the results of the other drainage basins. This is probably due to the orographic forcing, and also that the drainage basin is not extremely small. It thus seems that we are able to forecast the *average* precipitation over this drainage basin. The results do not differ much between the different resolutions. Again we would like to look in more detail how the forecast relates to the climate stations. To increase the number of observations, we are using a larger area than that of the drainage basin. The verification area chosen is shown in Figure 22, and it is homogeneous in the sence that the orography is important within the area. In the Figures 26 to 28 we show all climate observations for 24h precipitation (at 06Z) as compared to the sum of two forecasts of 12h precipitation, during the whole period from May 17 to 23.

PRECIP 22 KM RESOLUTION

FOREC

N=446, RMS=6.34, MAE=4.70

ME=-0.03, CORR=0.79

OBS
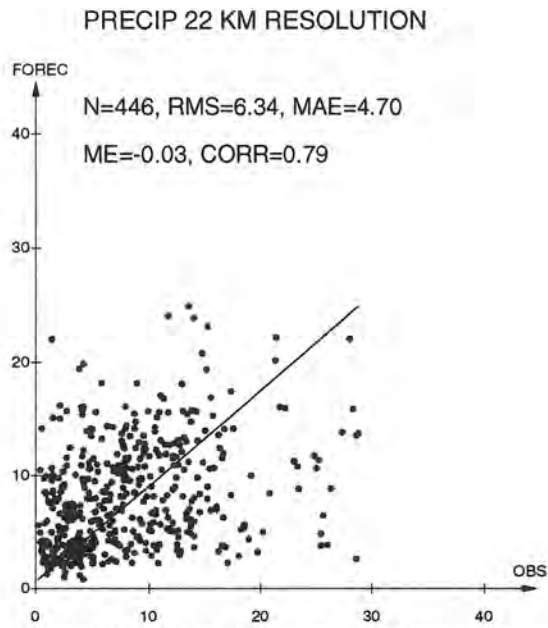
Figure 26. 22 km forecasts. Verifications against climate stations.

PRECIP 11 KM RESOLUTION

FOREC

N=446, RMS=6.63, MAE=4.91

ME=0.77, CORR=0.79

OBS
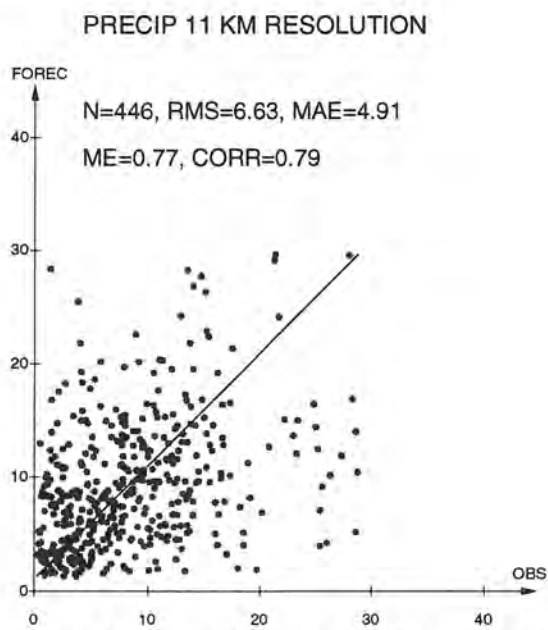
Figure 27. 11 km forecasts. Verifications against climate stations.
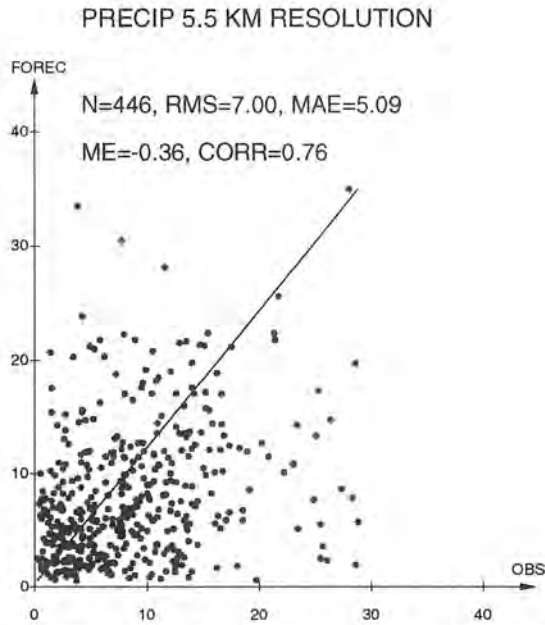
18

PRECIP 5.5 KM RESOLUTION

Figure 28. 5.5 km forecasts. Verifications against climate stations.

It can be seen from the figures that the three different resolutions of the forecasts give very similar results. It is even so, that the 22 km forecasts give a somewhat better skill. This indicates that the problem of estimating the precipitation is not solved by only using a higher horizontal resolution, within the present model framework. The parameterization of the convection is somewhat doubtful on these high resolution runs, and it might for example be better to try to resolve it (or at least to parameterize it in a different way), in a nonhydrostatic model framework.

5. Experiments with smoothed orography

We have seen from our experiments that the strength of the horizontal diffusion is of great importance for the precipitation pattern. The shorter waves have to be strongly damped, in order to avoid too noisy precipitation fields. It is reasonable to assume that a part of this noise is created by an orographic forcing that can not be handled by the model dynamics (Lander and Hoskins, 1997). Therefore we want to test the hypothesis that we could stay with less horizontal diffusion if instead the orography is smoothed. The 11 km orography has been smoothed by applying our horizontal diffusion scheme 20 iterations with a coefficient of $1.92 * 10^{12}$ and a timestep of 180 seconds. The response as a function of wavelength is shown in Figure 29. The 11 km orography before and after smoothing is shown in Figures 31 and 32 respectively.
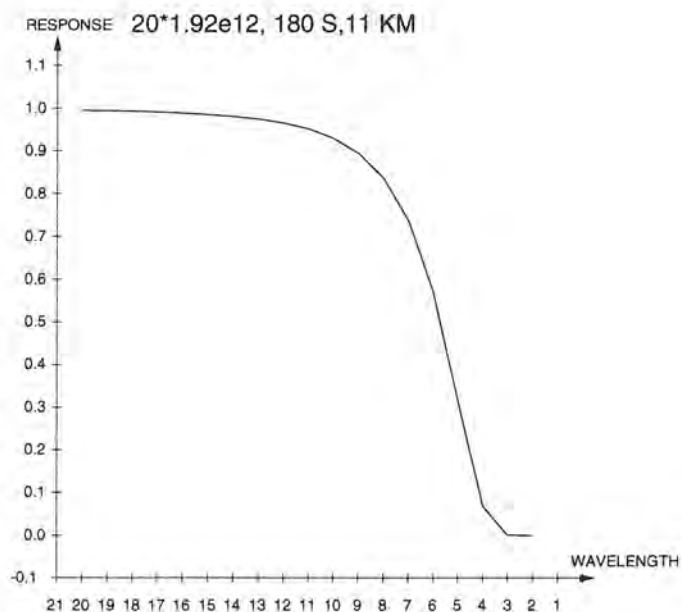
Figure 29. The response as a function of wavelength (unit=Δx) for orography smoothing.

We have been running all the forecasts in the same period in June 1996, with this smoothed orography. The coefficient of horizontal diffusion now has been the same as the less damped 11 km run in the earlier experiment, i.e. $6. * 10^{12}$. In Figure 33 the two 11 km 24 h accumulated precipitations are shown, together with the mesoscale analysed values. The results of the area integrated precipitations of the two different 11 km forecasts are comparable in quality. However now the kinetic energy spectrum is more realistic as shown in Figure 30. The kinetic energy spectrum of the more damped 11 km run (not shown), but with the original orography is very similar to that of Figure 11.
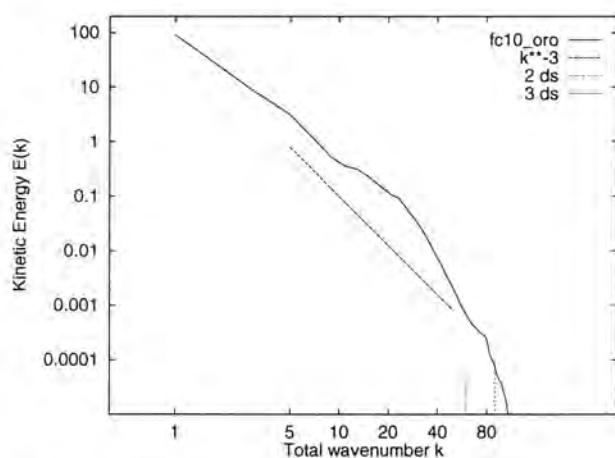

Figure 30. The kinetic energy spectrum for the 11 km forecast with smoothed orography.
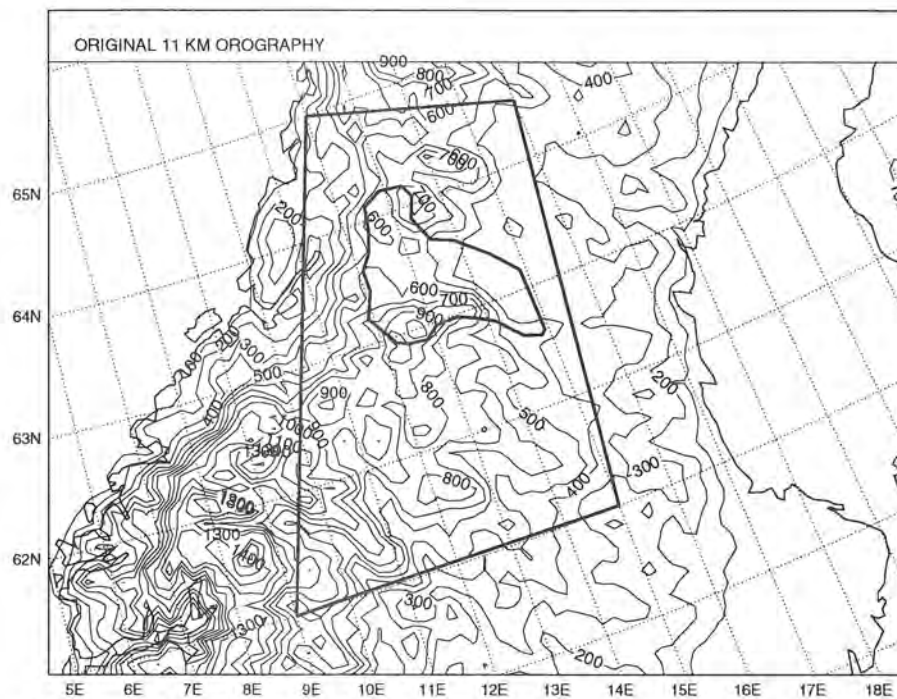
20

Figure 31. The 11 km original orography.
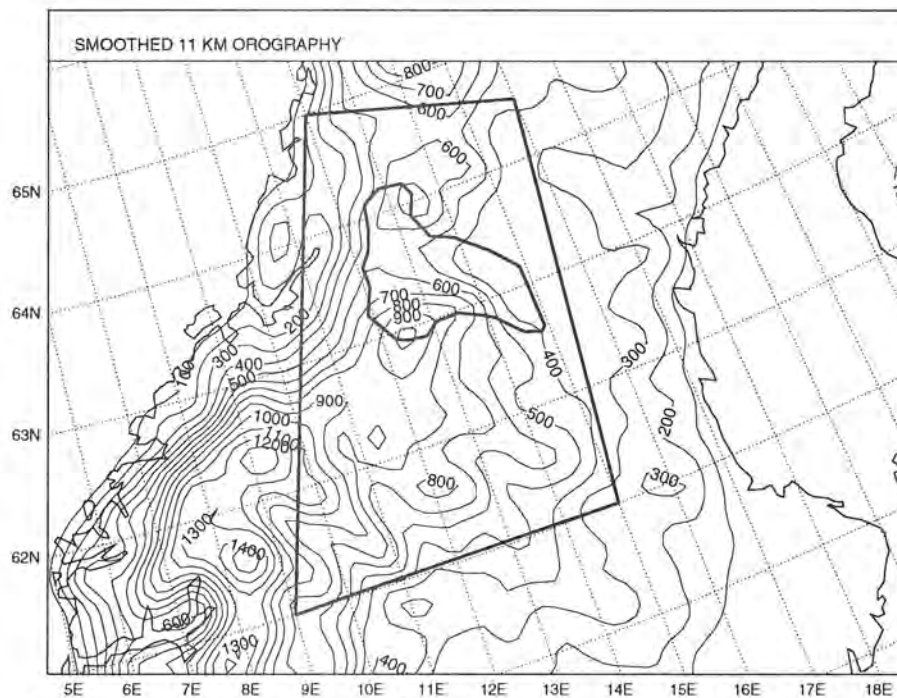
Figure 32. The 11 km smoothed orography.

INDALSÄLVEN JUNE 18-23
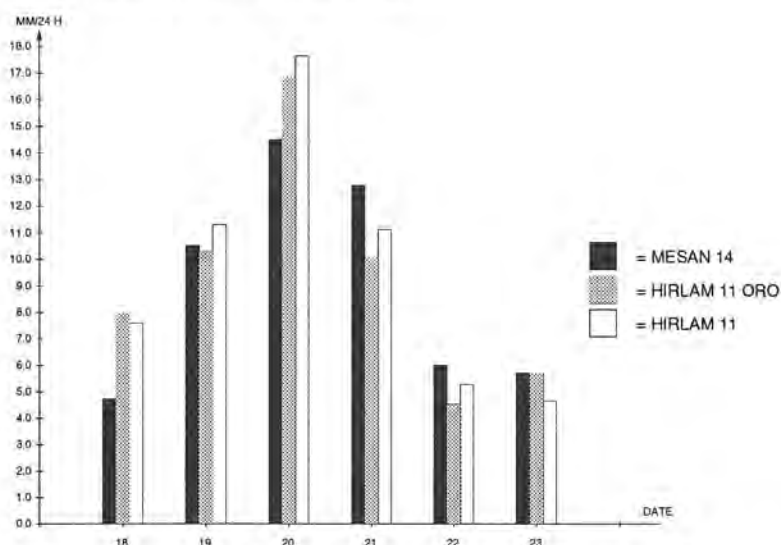
Figure 33. The 24h accumulated precipitation over Indalsälven drainage basin, during June 17-23 1996. Here 'ORO' means the cases with smoothed orography and less horizontal diffusion.

There are large differences in the precipitation pattern between the two 11 km runs. In Figures 34 and 35 are shown the results of 24 h accumulated precipitation summed up by two forecasts from +06h to +18h both in the case with original orography and also the smoothed orography case. Figure 36 shows the corresponding analysis.

Figure 34. The precipitation summed up from two 11 km +18h forecasts with original orography, valid at June 20 06Z.

22

Figure 35. The precipitation summed up from two 11 km +18h forecasts with smoothed orography, valid at June 20 06Z.

Figure 36. The 24h accumulated precipitation mesoscale analysis, valid at June 20 06Z.

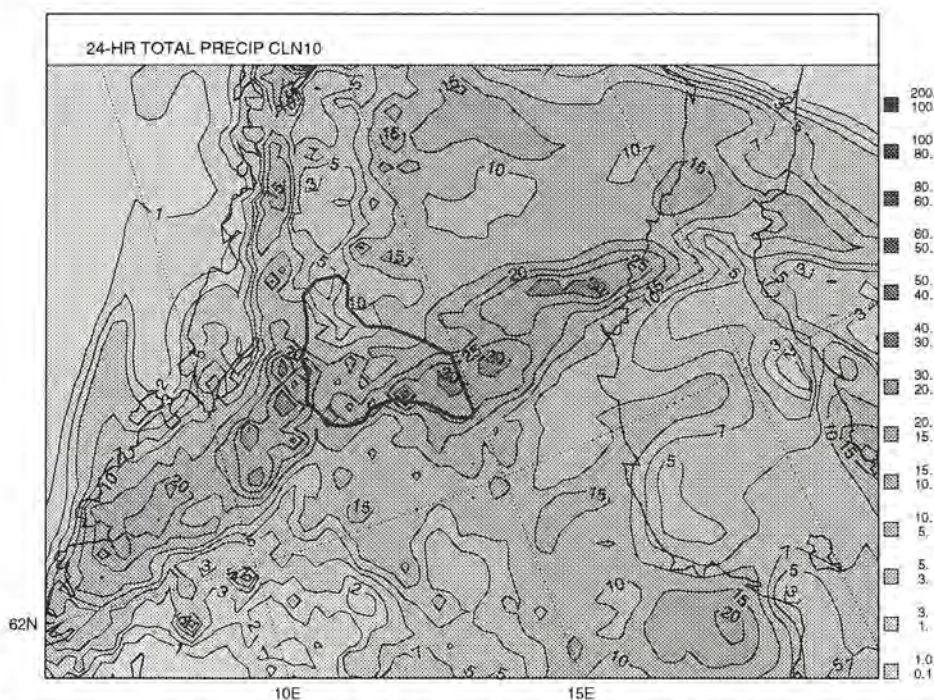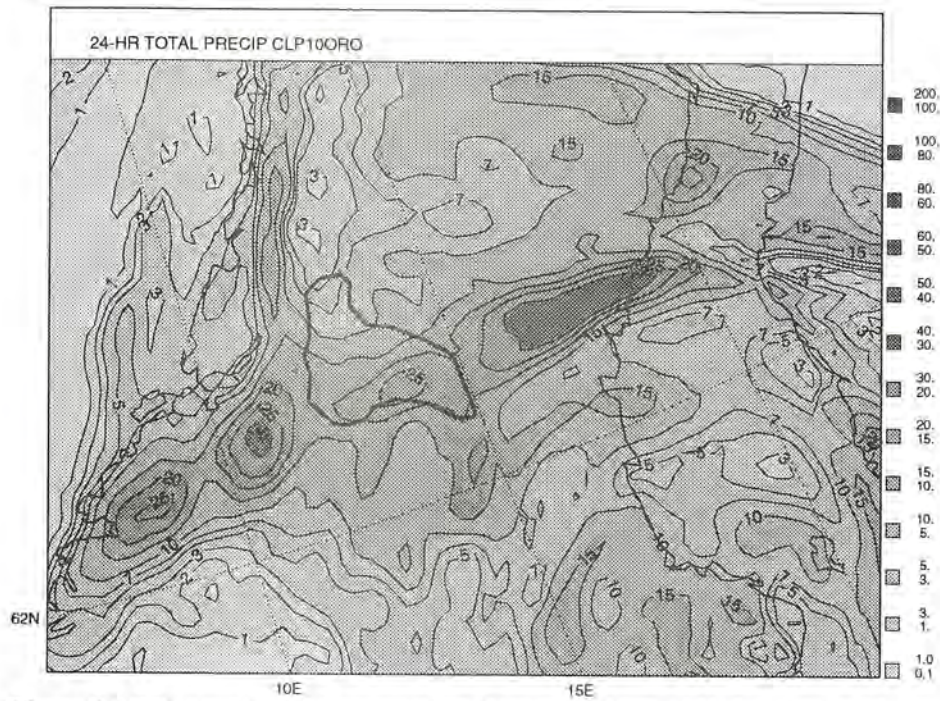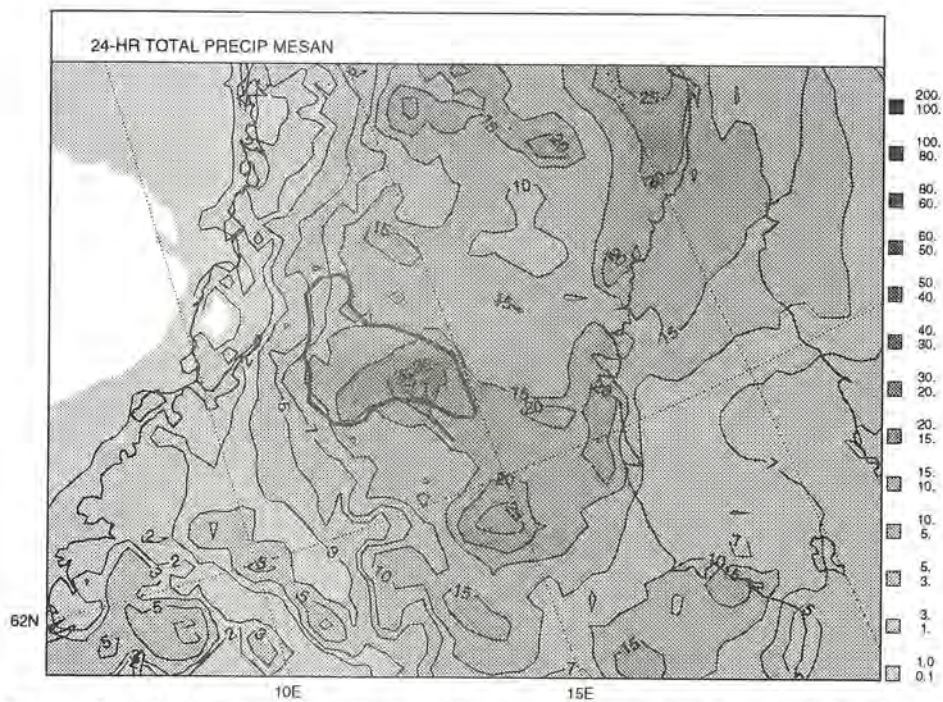It can be seen from the figures that the precipitation pattern is more noisy in the case with the original orography. The interpretation of this is that it is better not to feed the model from the lower boundary with small scale information and filter it strongly, with horizontal diffusion, but instead try to keep the energy spectrum more realistic and avoid the small scale orographic forcing. We have also made an experiment, following the ideas of Lander and Hoskins, where the tendencies in the free atmosphere, produced by the physical parameterization processes have been interpolated linearly from a grid with half resolution, i.e. 22 km grid. Also the accumulated precipitation has been interpolated in the same way. The corresponding precipitation from this experiment (the same smoothed orography) is depicted in Figure 37.
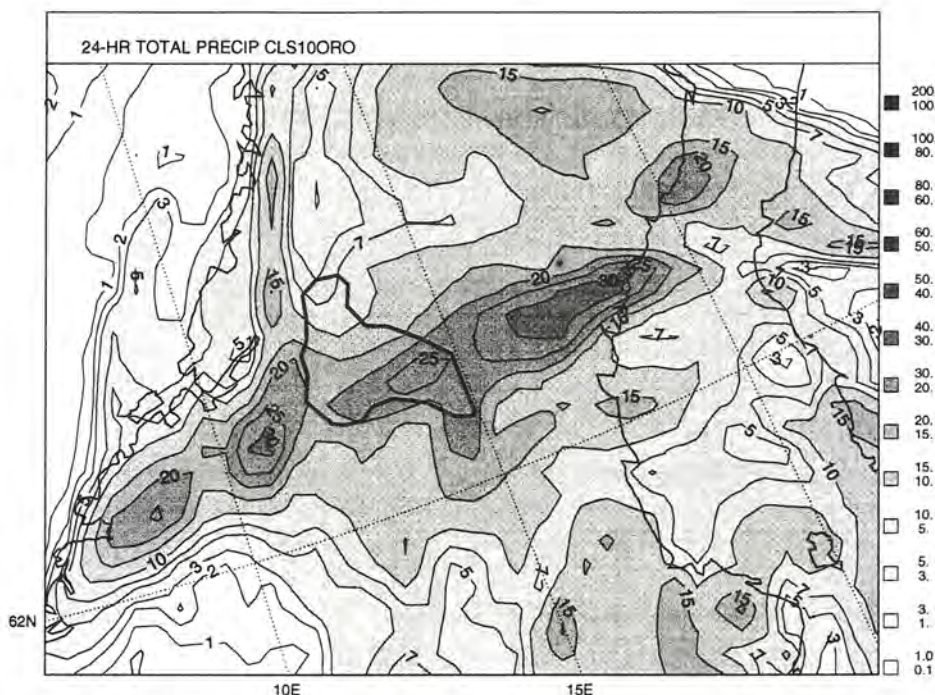
Figure 37. The 24h precipitation summed up from two 11 km +18h forecasts with smoothed orography and physics, valid at June 20 06Z.

The precipitation pattern of this approach is very similar to the case where only the orography is smoothed. This points towards a more economical way of integrating the model, since only one fourth of the points need to be included in the calculation of the physics, and at present about 70 % of the integration time is spent in the parameterization calculations. Of course some care has to be taken with the surface processes, and it is possible that a higher resolution interpretation of near surface variables is beneficial if such an approach is used.

6. Summary and conclusions

We have been running the HIRLAM model during two periods, May 20-25, 1996, and June 17-23, 1996. The precipitation has been estimated over drainage basins of different sizes. During the first period, the area of interest has been southern Sweden, an area which is not dominated by orographic effects. To see possible differences in more orographically forced cases, the second period has been evaluated over the Scandinavian mountain region. In both periods, the model has been run with 24 vertical levels and three different horizontal resolutions, 22, 11 and 5.5 km respectively.

The general results are that the HIRLAM model is capable of estimating the broad features of the precipitation, but has difficulties to estimate correct amounts over relatively small drainage basins in the case of weak orographical forcing. When the flow is strongly influenced by orography, the results look much better, and the results indicate that we are able to forecast the average precipitation over a reasonable large drainage basin. In none of the periods, improvments could be seen by increasing the horizontal resolution. One reason for the lack of improvements could be that the parameterization is sensitive to the resolution. Also the spinup problem, which in turn could be related to the size of the integration area, and to the time resolution of the boundaries, could be important.

An important complication is that the resulting precipitation pattern is strongly dependent on the magnitude of the horizontal diffusion. In a case study of the first period, we found that a strongly damped 11 km run was slightly better, than the version which produces a more realistic kinetic energy spectrum. The 5 km forecasts need also to be subject to large horizontal diffusion, in order to control the noise in the precipitation pattern.

We have also tried to avoid the problem with too strongly damped forecasts, by instead smoothing the orography. The precipitation now looks more realistic, and at the same time also the kinetic energy spectra are better. An experiment where, in addition, the physical parameterizations have been evaluated on a grid of half the resolution, as that of the dynamics shows almost exactly the same precipitation pattern.

Since the precipitation, at least in cases of weak orography, is determined by the detailed description of the weather systems, i.e. the development is critically dependent on the initial conditions, the exact position in time and space is difficult to forecast. This means that we can produce different precipitations by changing the initial conditions, well within the analysis error. This points, in order to make forecasts of precipitation over specific drainage basins, towards an approach based on ensemble forecasting. The results should be possible to interpret as probabilities for precipitation over the actual basins.

7. Acknowledgements

8. References

Gustafsson, N., Mc Donald, A., 1996: A Comparison of the HIRLAM Gridpoint and Spectral Semi-Lagrangian Models, Mon. Wea. Rev., 124, pp 2008-2022.

Häggmark, L., Ivarsson, K.I., Olofsson, P.O., 1997: MESAN, Mesoskalig analys, RMK 75, SMHI, Norrköping, Sweden

Källén, E., 1996 (editor): HIRLAM Documentation Manual, system 2.5, (Available from SMHI, Norrköping, Sweden)

Kuo,J.L., 1974: Further studies of the parameterization of the influence of cumulus convection on large-scale flow. J. Atmos. Sci., 31, 1232-1240.

Lander, J., Hoskins, B., 1997: Believable Scales and Parameterizations in a Spectral Transform Model, Mon. Wea. Rev. 125, 292-303.

Lindström, G., Johansson, B., Persson, M., Gardelin, M., Bergström, S., 1996: Development and test of the distributed HBV-96 hydrological model. Accepted for publication in Journal of Hydrology.

Sundqvist, H., Berge, E. and Kristjansson, J. E., 1989: Condensation and cloud parameterization studies with a mesoscale numerical weather prediction model. Mon. Wea. Rev. 117, 1641-1657.

Sundqvist, H., 1993: Parameterization of clouds in large scale numerical models, in Aerosol-Cloud-Climate Interactions, editted by P.V. Hobbs, pp. 175-203, Academic Press, Inc.

SMHIs publications

SMHI publishes six report series. Three of these, the R-series, are intended for international readers and are in most cases written in English. For the others the Swedish language is used.

Names of the Series	Published since
RMK (Report Meteorology and Climatology)	1974
RH (Report Hydrology)	1990
RO (Report Oceanography)	1986
METEOROLOGI	1985
HYDROLOGI	1985
OCEANOGRAFI	1985

Earlier issues published in serie RMK

1 Thompson, T., Udin, I., and Omstedt, A. (1974)
Sea surface temperatures in waters surrounding Sweden.

2 Bodin, S. (1974)
Development on an unsteady atmospheric boundary layer model.

3 Moen, L. (1975)
A multi-level quasi-geostrophic model for short range weather predictions.

4 Holmström, I. (1976)
Optimization of atmospheric models.

5 Collins, W.G. (1976)
A parameterization model for calculation of vertical fluxes of momentum due to terrain induced gravity waves.

6 Nyberg, A. (1976)
On transport of sulphur over the North Atlantic.

7 Lundqvist, J.-E., and Udin, I. (1977)
Ice accretion on ships with special emphasis on Baltic conditions.

8 Eriksson, B. (1977)
Den dagliga och årliga variationen av temperatur, fuktighet och vindhastighet vid några orter i Sverige.

9 Holmström, I., and Stokes, J. (1978)
Statistical forecasting of sea level changes in the Baltic.

10 Omstedt, A., and Sahlberg, J. (1978)
Some results from a joint Swedish-Finnish sea ice experiment, March, 1977.

11 Haag, T. (1978)
Byggnadsindustrins väderberoende, seminarieuppsats i företagsekonomi, B-nivå.

12 Eriksson, B. (1978)
Vegetationsperioden i Sverige beräknad från temperaturobservationer.

13 Bodin, S. (1979)
En numerisk prognosmodell för det atmosfäriska gränsskiktet, grundad på den turbulenta energiekvationen.

14 Eriksson, B. (1979)
Temperaturfluktuationer under senaste 100 åren.

15 Udin, I., och Mattisson, I. (1979)
Havsis- och snöinformation ur datorbearbetade satellitdata - en modellstudie.

16 Eriksson, B. (1979)
Statistisk analys av nederbördsdata. Del I. Arealnederbörd.

17 Eriksson, B. (1980)
Statistisk analys av nederbördsdata. Del II. Frekvensanalys av månadsnederbörd.

18 Eriksson, B. (1980)
Årsmedelvärden (1931-60) av nederbörd, avdunstning och avrinning.

19 Omstedt, A. (1980)
A sensitivity analysis of steady, free floating ice.

20 Persson, C., och Omstedt, G. (1980)
En modell för beräkning av luftföroreningars spridning och deposition på mesoskala.

21 Jansson, D. (1980)
Studier av temperaturinversioner och vertikal vindskjuvning vid Sundsvall-Härnösands flygplats.

22 Sahlberg, J., and Törnevik, H. (1980)
A study of large scale cooling in the Bay of Bothnia.

23 Ericson, K., and Hårsmar, P.-O. (1980)
Boundary layer measurements at Klockrike. Oct. 1977.

24 Bringfelt, B. (1980)
A comparison of forest evapotranspiration determined by some independent methods.

25 Bodin, S., and Fredriksson, U. (1980)
Uncertainty in wind forecasting for wind power networks.

26 Eriksson, B. (1980)
Graddagsstatistik för Sverige.

27 Eriksson, B.(1981)
Statistisk analys av nederbördsdata. Del III. 200-åriga nederbördsserier.

28 Eriksson, B. (1981)
Den "potentiella" evapotranspirationen i Sverige.

29 Pershagen, H. (1981)
Maximisnödjup i Sverige (perioden 1905-70).

30 Lönnqvist, O. (1981)
Nederbördsstatistik med praktiska tillämpningar.
(Precipitation statistics with practical applications.)

31 Melgarejo, J.W. (1981)
Similarity theory and resistance laws for the atmospheric boundary layer.

32 Liljas, E. (1981)
Analys av moln och nederbörd genom automatisk klassning av AVHRR-data.

33 Ericson, K. (1982)
Atmospheric boundary layer field experiment in Sweden 1980, GOTEX II, part I.

34 Schoeffler, P. (1982)
Dissipation, dispersion and stability of numerical schemes for advection and diffusion.

35 Undén, P. (1982)
The Swedish Limited Area Model. Part A. Formulation.

36 Bringfelt, B. (1982)
A forest evapotranspiration model using synoptic data.

37 Omstedt, G. (1982)
Spridning av luftförorening från skorsten i konvektiva gränsskikt.

38 Törnevik, H. (1982)
An aerobiological model for operational forecasts of pollen concentration in the air.

39 Eriksson, B. (1982)
Data rörande Sveriges temperaturklimat.

40 Omstedt, G. (1984)
An operational air pollution model using routine meteorological data.

41 Persson, C., and Funkquist, L. (1984)
Local scale plume model for nitrogen oxides. Model description.

42 Gollvik, S. (1984)
Estimation of orographic precipitation by dynamical interpretation of synoptic model data.

43 Lönnqvist, O. (1984)
Congression - A fast regression technique with a great number of functions of all predictors.

44 Laurin, S. (1984)
Population exposure to So and NO_x from different sources in Stockholm.

45 Svensson, J. (1985)
Remote sensing of atmospheric temperature profiles by TIROS Operational Vertical Sounder.

46   Eriksson, B. (1986)
Nederbörds- och humiditetsklimat i
Sverige under vegetationsperioden.

47   Taesler, R. (1986)
Köldperioden av olika längd och före-
komst.

48   Wu Zengmao (1986)
Numerical study of lake-land breeze over
Lake Vättern, Sweden.

49   Wu Zengmao (1986)
Numerical analysis of initialization
procedure in a two-dimensional lake
breeze model.

50   Persson, C. (1986)
Local scale plume model for nitrogen
oxides. Verification.

51   Melgarejo, J.W. (1986)
An analytical model of the boundary layer
above sloping terrain with an application to
observations in Antarctica.

52   Bringfelt, B. (1986)
Test of a forest evapotranspiration model.

53   Josefsson, W. (1986)
Solar ultraviolet radiation in Sweden.

54   Dahlström, B. (1986)
Determination of areal precipitation for the
Baltic Sea.

55   Persson, C. (SMHI), Rodhe, H. (MISU),
De Geer, L.-E. (FOA) (1986)
The Chernobyl accident - A meteorologi-
cal analysis of how radionucleides reached
Sweden.

56   Persson, C., Robertson, L. (SMHI), Grenn-
felt, P., Kindbom, K., Lövblad, G., och
Svanberg, P.-A. (IVL) (1987)
Luftföroreningsepisoden över södra
Sverige 2 - 4 februari 1987.

57   Omstedt, G. (1988)
An operational air pollution model.

58   Alexandersson, H., Eriksson, B. (1989)
Climate fluctuations in Sweden
1860 - 1987.

59   Eriksson, B. (1989)
Snödjupsförhållanden i Sverige -
Säsongerna 1950/51 - 1979/80.

60   Omstedt, G., Szegö, J. (1990)
Människors exponering för luftförore-
ningar.

61   Mueller, L., Robertson, L., Andersson, E.,
Gustafsson, N. (1990)
Meso-γ scale objective analysis of near
surface temperature, humidity and wind,
and its application in air pollution model-
ling.

62   Andersson, T., Mattisson, I. (1991)
A field test of thermometer screens.

63   Alexandersson, H., Gollvik, S.,
Meuller, L. (1991)
An energy balance model for prediction of
surface temperatures.

64   Alexandersson, H., Dahlström, B. (1992)
Future climate in the Nordic region -
survey and synthesis for the next century.

65   Persson, C., Langner, J., Robertson, L.
(1994)
Regional spridningsmodell för Göteborgs
och Bohus, Hallands och Älvsborgs län. (A
mesoscale air pollution dispersion model
for the Swedish west-coast region. In
Swedish with captions also in English.)

66   Karlsson, K.-G. (1994)
Satellite-estimated cloudiness from NOAA
AVHRR data in the Nordic area during
1993.

67   Karlsson, K-G. (1996)
Cloud classifications with the SCANDIA
model.

68   Persson, C., Ullerstig, A. (1996)
Model calculations of dispersion of lindane
over Europe. Pilot study with comparisons
to measurements around the Baltic Sea and
the Kattegat.

69   Langner, J., Persson, C., Robertson, L.,
and Ullerstig, A. (1996)
Air pollution Assessment Study Using the
MATCH Modelling System. Application
to sulfur and nitrogen compounds over
Sweden 1994.

70   Robertson, L., Langner, J., Engardt, M.
(1996)
MATCH - Meso-scale Atmosperic
Transport and Chemistry modelling
system.

71   Josefsson W. (1996)
Five years of solar UV-radiation
monitoring in Sweden.

72   Persson, C., Ullerstig, A., Robertson, L., Kindbom, K., Sjöberg, K. (1996)
The Swedish Precipitation Chemistry Network. Studies in network design using the MATCH modelling system and statistical methods.

73   Robertson, L. (1996)
Modelling of anthropogenic sulfur deposition to the African and South American continents.

74   Josefsson, W. (1996)
Solar UV-radiation monitoring 1996.

75   Häggmark, L., Ivarsson, K.-I. (SMHI), Olofsson, P.-O. (Militära vädertjänsten). (1996)
MESAN - Mesoskalig analys.

76   Bringfelt, B, Backström, H, Kindell, S, Omstedt, G, Persson, C, Ullerstig, A.
Calculations of PM-10 concentrations in Swedish cities- Modelling of inhalable particles

SMHI